Statistical significance of geomagnetic diurnal variation anomalies prior to worldwide earthquakes

Khairul Adib Yusof[1,2], Mardina Abdullah[2,3], Nurul Shazana Abdul Hamid[2,4], Suaidi Ahadi[5], and Essam Ghamry[6,7]

[1] Department of Physics, Faculty of Science, Universiti Putra Malaysia, Malaysia
[2] Space Science Center, Institute of Climate Change, Universiti Kebangsaan Malaysia, Malaysia
[3] Department of Electrical, Electronic and Systems Engineering,
Faculty of Engineering and Built Environment, Universiti Kebangsaan Malaysia
[4] Department of Applied Physics, Faculty of Science and Technology,
Universiti Kebangsaan Malaysia
[5] Department of Geophysics, Indonesian Agency for Meteorology, Climatology and Geophysics,
Jakarta, Indonesia
[6] National Research Institute of Astronomy and Geophysics, Helwan 11421, Cairo, Egypt
[7] International Center for Space Weather Science and Education,
Kyushu University, Fukuoka 819-0395, Japan

Correspondence: Khairul Adib Yusof (email: adib.yusof@upm.edu.my)

Received: 12 August 2021; Accepted: 03 November 2021; Published: 30 November 2021

Abstract

The anomalous behavior of geomagnetic diurnal variation was reported by prior studies several months before the great 2011 Tohoku earthquake. In order to be further developed for a reliable earthquake prediction system, the statistical significance of such anomalies needs to be verified through a multiple-events study. In this paper, 157 past earthquakes that happened from the year 2000 until 2019 around the world were studied by utilizing vast low-resolution (1-min sampling period) geomagnetic field data. The Diurnal Variation Range Ratio (DVRR) method was employed to identify the disappearance of typical diurnal variation at magnetometer stations near epicenters, whereas superposed epoch analysis was the statistical tool used to reveal the periodicity of anomaly appearances. This research found that the number of anomalies in all three geomagnetic field components (i.e., northward, eastward, and vertical) increased significantly only before the earthquakes starting from around one month prior. The significant increments were not simultaneous, instead there were temporal lags between the components. Several mechanisms were proposed to elucidate the generation of the anomalies as well as to explain the observed temporal lags. Through the analysis, it could be concluded that the statistical significance of the anomalies could be verified. It was possible that the anomalies were the earthquake precursors.

Keywords: Earthquake, geomagnetic diurnal variation, magnetometer data, seismo-electromagnetics, SuperMAG network, superposed epoch analysis

Introduction

Shear strain and stress that are slowly accumulated in the Earth's crustal layer could result in sudden energy release and seismic wave generation as well as causing shaking and/or ground displacements; this phenomenon is better known as earthquake. Earthquakes occur approximately 500,000 times per year, where minor earthquakes happen nearly all the time in high seismic zones especially California, Indonesia, Japan, and Italy (Hayakawa, 2015). Due to the great impacts of earthquakes in terms of casualty and property destruction, the earthquake prediction field has been gaining pace since the last century, leading to 40 earthquake precursor candidates being considered and evaluated by the Sub-Commission on Earthquake Prediction of the International Association for Seismology and Physics of the Earth's Interior (IASPEI) in 1980s (Jordan et al., 2011). Among the candidates, anomalies in the geomagnetic field are one of the types that was frequently discussed and has been continually researched (Hayakawa, 2018). This situation led to the introduction of various detection techniques like polarization ratio (Yusof et al., 2021), Ultra-Low Frequency (ULF) depression (Schekotov et al., 2020), and principal component analysis (Zhu et al., 2019). Additionally, geomagnetic anomalies could also be manifested and detected in the form of diurnal variation (Xu et al., 2013), which is the focus of the present study.

The periodic fluctuation of geomagnetic field intensity over 24 hours is referred to as diurnal variation of the field that largely depends on the solar quiet current system produced by magnetospheric and ionospheric currents. Although the variation is influenced by various main sources, other sources including the minor ones through the investigation on the behavior of the variations still can be identified. For example, during the presence of inhomogeneous ionospheric currents, it is common to observe short-periodic disturbances lasting for a several hours to a few days (Hamid et al., 2021). Additionally, solar-terrestrial disturbances due to geomagnetic storms are possible to be discerned by observing Planetary (*ap*) and Disturbance Storm-Time (*Dst*) indices, which are some examples of global geomagnetic indices (Yusof et al., 2020). Likewise, changes of conductivity occurring in the underground before large earthquakes may induce diurnal variation anomalies in close proximity to the epicenter, even though their appearances are usually relatively inconspicuous and can be masked by the more dominant Earth's main field.

Therefore, a signal processing technique that is capable in emphasizing and highlighting the anomalies is needed. The effectiveness of Diurnal Variation Range Ratio (DVRR) method has been demonstrated by prior studies in detecting pre-earthquake geomagnetic diurnal variation anomalies (Han et al., 2015; Han et al., 2016; Xu et al., 2013). However, past studies usually investigated only a few earthquakes where the study area was limited to a certain seismoactive region. This practice may have caused a question – were the observed anomalies actually earthquake precursors or did they happen by chance? (Masci & Thomas, 2015). In order to answer the question, comprehensive statistical analyses that include a large number of earthquakes in multiple regions around the world can be done. Prior studies have conducted similar analyses on different types of anomalies, for instance, the Superposed Epoch Analysis (SEA) has been adopted to determine whether the reported ULF anomalies appearing before earthquakes were statistically significant (Han et al., 2014; Hattori et al., 2013). SEA was specifically used in the studies because it can uncover obscure periodicities hidden in multiple time series (Singh & Badruddin, 2006). While, the DVRR method has the edge over ULF methods since the former only needs low-resolution data whereas high-resolution data (i.e., 1-Hz sampling frequency or higher) are necessary for the latter to be implemented. As low-resolution data are readily and freely accessible via online databases, it is more viable to conduct extensive studies by utilizing the data.

This present study aims to utilize long-term low-resolution geomagnetic data to apply the DVRR method alongside the SEA for a statistical analysis of pre-earthquake diurnal variation anomaly detection. Results obtained from the analysis will verify the anomalies appearing prior to earthquakes in terms of statistical significance. As similar studies have not been done before, this study will also explore the possible generation and propagation mechanisms of pre-earthquake diurnal variation to explain our observations.

Data and methodology

1-min sampling period geomagnetic field data utilized in this study were obtained from the SuperMAG database (www.supermag.jhuapl.edu) (Chi et al., 2013; Clauer et al., 2014; Engebretson et al., 1995; Gjerloev, 2012; Lichtenberger et al., 2013; Love & Chulliat, 2013; Mann et al., 2008; Tanskanen, 2009; Yumoto, 2001). The spatial and temporal coverages of this study were extensive where data collected at 138 magnetometer stations around the world within the period of study, which was set between the year 1999 and 2019, were involved. The stations are either induction-coil or vector fluxgate types with a three-axis configuration that collect data consisting of three components, referred to as *N*, *E*, and *Z*, corresponding to northward, eastward, and vertical components in the geomagnetic coordinate (Gjerloev, 2012). Additionally, Planetary (*ap*) and Disturbance Storm-Time (*Dst*) global geomagnetic indices data that were acquired through the NASA OMNIWeb Service (www.omniweb.gsfc.nasa.gov) were also analyzed. Since derivations of the indices involve geomagnetic field measurements at observatories situated near the mid-latitudes and the equator, respectively, their utilization provided this study with overall conditions of the global geomagnetic activity level and the presence of solar-terrestrial disturbances (Rostoker, 1972). The days with the intensity of the indices reaching predefined threshold values of $ap > 27$ nT or $Dst < 30$ nT were considered 'disturbed', hence, any geomagnetic field anomalies observed during these days were eliminated. Besides, earthquake event details that happened within the period of study and satisfied the criteria of hypocentral depth, $h \leq 200$ km, magnitude, $M \geq 6.0$, and epicentral distance, $d \leq 190$ km were acquired from the European-Mediterranean Seismological Centre catalog (www.emsc-csem.org). Note that d for each earthquake was measured from any of the stations. In order to implement the DVRR method, datasets from at least one station pair were needed for every earthquake event; the stations were referred to as 'near' and 'far' stations. Therefore, 479 station pairs, which were made up of 92 individual stations, were algorithmically determined based on their distances from 157 earthquakes, providing $n = 479$ for the statistical analysis using the SEA. The earthquakes and stations are illustrated in Fig. 1 as red circles and blue triangles, respectively.

The DVRR method aims to amplify pre-earthquake diurnal variation anomalies in the geomagnetic field (Han et al., 2015; Xu et al., 2013; Yusof et al., 2019). In this study, near and far stations have epicentral distances of $d \leq 190$ km and $600 \text{ km} < d < 1000$ km, respectively. Additionally, far stations that had other earthquakes happened within 190 km during the observation period were excluded to isolate the seismic effects to the main earthquake only. Diurnal variation ranges of the N component at the far station, $\Delta N_{far,i}$ on the i-th day were divided by ranges at the near station, $\Delta N_{near,i}$ – this parameter is known as the daily range ratio, $R_{N,i}$. The parameter might fluctuate randomly, hence, its 15-day moving average, $\bar{R}_N$ was computed to observe its long-term trend more clearly. The calculations were done as follows:

© 2021, e-ISSN 2682-7727 https://doi.org/10.17576/geo-2021-1704-25

$$R_{N,i} = \frac{\Delta N_{far}}{\Delta N_{near}}, \quad \bar{R}_{N,i} = \frac{1}{w}\sum_{i-C}^{i+F} R_{N,i}$$

where: w is the moving average window size (i.e., $w = 15$), whereas F and C refer to the floor and ceiling of $0.5(w-1)$, respectively. Similar processes were performed on the E and Z components as well where the period starting from 55 days before until 55 days after each earthquake day (i.e., ±55 days) was observed. Then, an 'anomaly' was identified if the daily value, $\bar{R}_i$ of the component surpasses the mean plus or minus two times the standard deviation ($\mu \pm k\sigma$) of the whole period of observation, which implies that the anomaly is outside the 95% of the normally distributed dataset (Han et al., 2015).

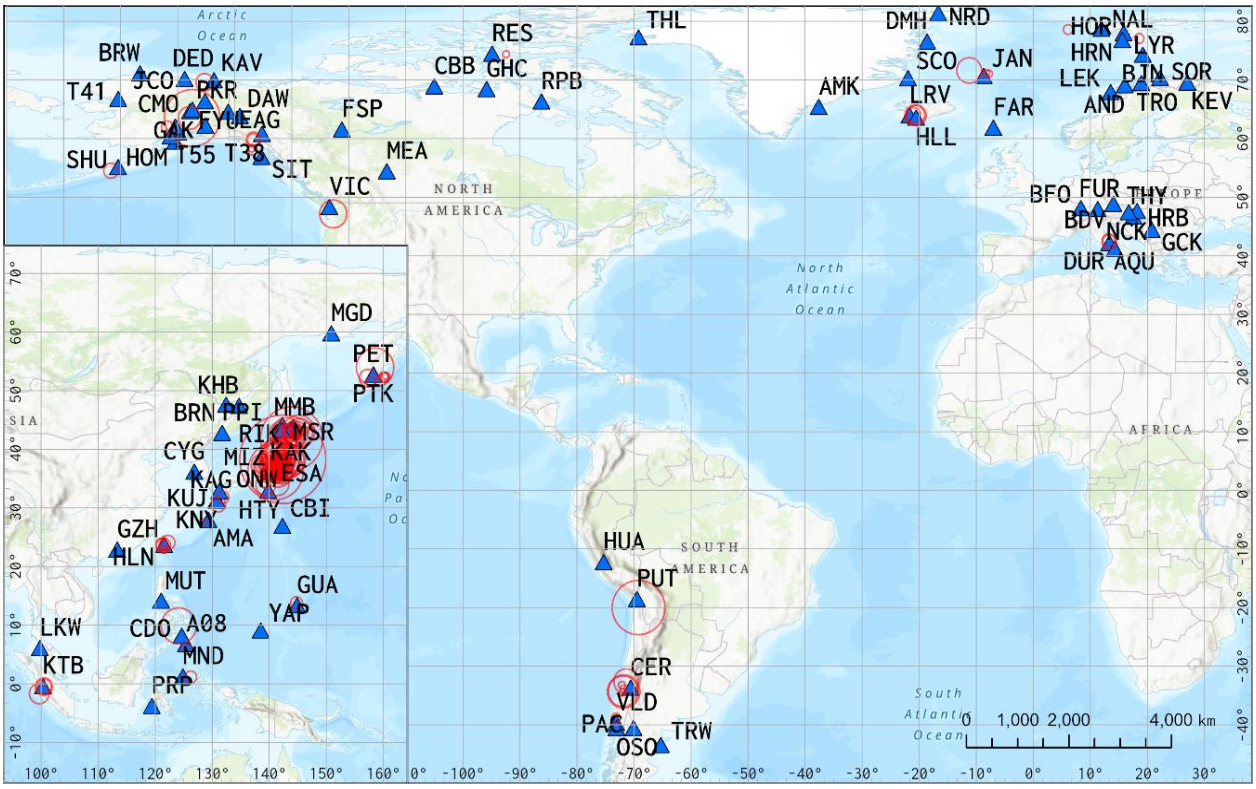

Figure 1. The maps showing the studied earthquakes and stations, represented as red circles and blue triangles, respectively, in America and Europe (main map) as well as Asia (inset map). The radii of the circles are proportional to the earthquake magnitudes.

Through the implementation of the SEA, a total of n binary temporal observations and $y(t)$ of a parameter in respect to an event of reference, t_r were composited. In the present study, $\bar{R}$ and each studied earthquake were set as the parameter and event of reference, respectively. The analysis is based on the assumption that the signals related to the event will stand out from the background signatures, which will be averaged out due to the composition. The signal occurrence sum, $s(t)$ was computed as follows:

$$s(t) = \sum_{i=1}^{n} y_i(t - t_r)$$

where: $y_i(t-t_r)$ refers to the observation time series that has been shifted relative to the earthquake day, in this case by positioning the earthquake day at the center of the time series (i.e., day 0) (Samson & Yeung, 1986). In this study, every anomaly appearance was counted and the day number, *i* of the appearance was recorded for every available near–far station pair ($n = 479$), then the counts were added up to get the total anomaly count for each of the 111 days. Finally, an anomaly count was regarded as significant if it surpasses the mean plus two standard deviations ($\mu + 2\sigma$) (Hattori et al., 2013).

Results and discussion

Before discussing the overall results of statistical analysis, it was important to understand the variation of raw geomagnetic field data. Fig. 2 exemplifies the field intensity in nT measured at Kakioka (KAK) and Memambetsu (MMB), Japan stations from 16 days before until the day of M6.1 Honshu, Japan earthquake on 13th of May 2011, where for this event, KAK and MMB act as the near and far stations. Based on the values of the global geomagnetic indices, disturbed days were identified as shown by the magenta shade in Fig. 2. The geomagnetic field data of a component measured at two close stations are known to closely correspond with each other. Besides, solar disturbances like geomagnetic storms would cause similar global effects at both stations (Potirakis et al., 2017). This behavior was clearly apparent in Fig. 2 during both quiet (unshaded) and disturbed (shaded) days, with the exception of a three-day period in the Z component at the near station; the period is highlighted by the yellow dashed line rectangle in Fig. 2e. Unlike its far station counterpart in Fig. 2f, the intensity of the field component during the highlighted period showed less variations, starting from –9 until the end of –7 days in respect to the earthquake day. The anomalous disappearance of diurnal variation specifically in the Z component prior to a sizeable earthquake is consistent with findings by prior studies (e.g., Han et al., 2016). Similar anomalies during other periods and before other earthquakes were searched by employing the DVRR method that can emphasize the appearance of anomalies.

DVRR analysis results of all studied earthquakes were merged through the SEA. Since anomalies that may have possible association with many earthquakes occurring in different periods might appear on different days relative to their respective earthquakes, an analysis accumulated throughout a longer period was essential to uncover any noteworthy observations. For this purpose, 5-day counts were found to be useful (Han et al., 2014; Hattori et al., 2013), which are simply the summations of 1-day counts throughout five consecutive days. Fig. 3 shows SEA results based on $\bar{R}$ where the 5-day counts (bars) and statistical significance based on $\mu + 2\sigma$ thresholds (dashed lines) are shown in blue, orange, and yellow for N, E, and Z components, respectively. Note that the *x*-axis tick label to the left of each bar group indicates the lower boundary of the 5-day count, e.g., the leftmost bar group starts at day –55 and ends at day –51. It was apparent from Fig. 2 that the anomaly counts for the N component (blue bars) significantly increased throughout days –30 to –26 and –20 to –16. The other two components exhibited a similar observation, except the increases were closer in time to the earthquake day, which were throughout days –15 to –11 for the E (orange bars), whereas –10 to –6 and –5 to –1 for Z components (yellow bars).

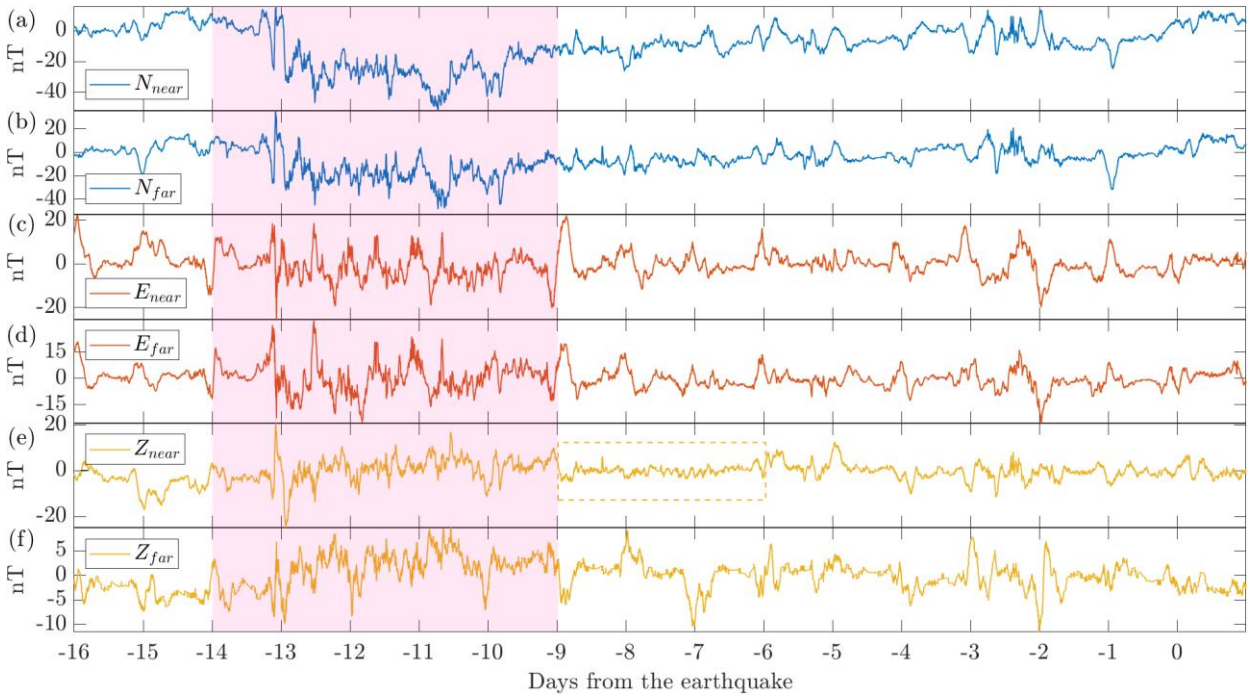

Figure 2. Raw geomagnetic field intensity (nT) measured at a pair of near and far stations for *N*, *E*, and *Z* components from 16 days before until the day of earthquake. Disturbed days are shaded magenta, while the dashed line rectangle in (e) highlights the disappearance of geomagnetic variation.

Furthermore, it was clear that the Z anomaly count increased at a slower rate before the earthquake day (solid black line), but the decrease was steeper after the highest count in comparison with both N and E components. A minor increase was also seen specifically in the Z component following the initial increase, although the minor increase was below the statistical significance value. Since the incorporation of the SEA into DVRR method has never been done before, a comparison could only be made indirectly with Hattori et al. (2013) that performed SEA on the Z component to identify pre-earthquake anomalous energy enhancements within the ULF range. The behavior of the Z variation in the present study is in agreement with their study where a gradual increase during the pre-earthquake period followed by a steep decrease during the post-earthquake period then a final minor increase was observed. However, since the observations for both N and E components were not reported in that study, no comparisons could be made for both components. As previously explained, disturbances from external sources have been removed by discarding anomalies during disturbed periods as well as calculating the near–far station ratio. Therefore, we could safely say that the detected N and E anomalies probably came from the same source and were generated by the same mechanism that caused the anomalies in the Z component, except there were approximately 5-day temporal lags between the components. Hence, it could be concluded that the anomalies observed through the DVRR method might have association with the earthquakes that followed.

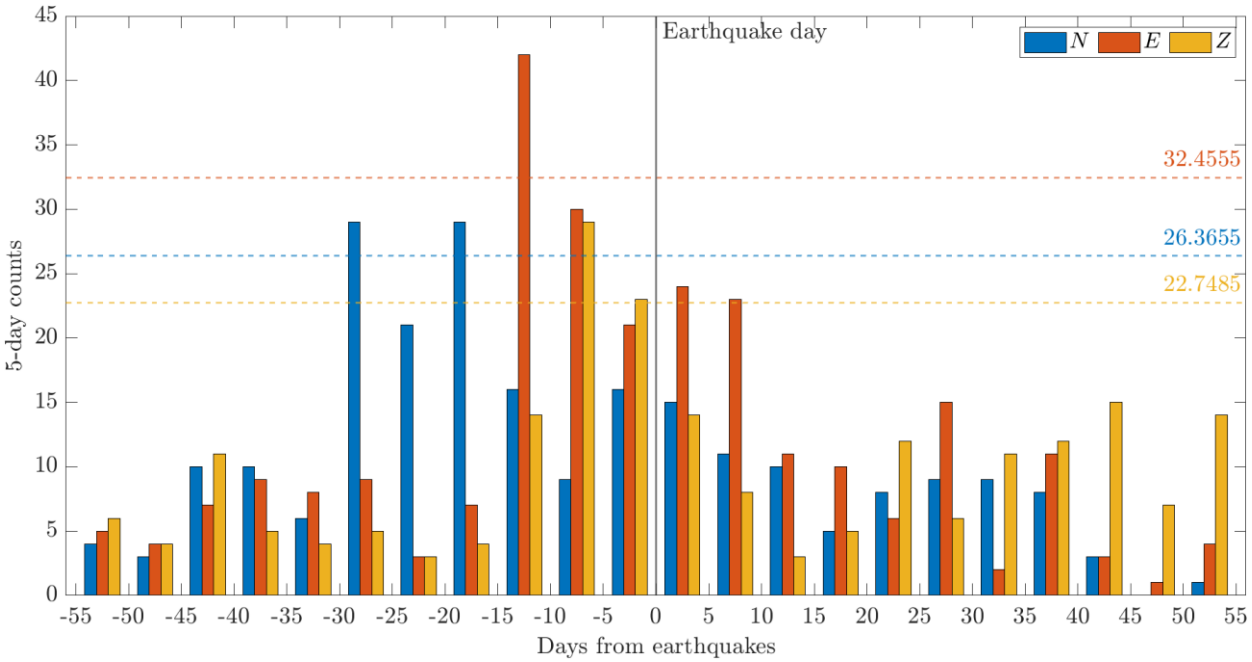

Figure 3. SEA results based on $\bar{R}$ where 5-day counts and their respective $\mu + 2\sigma$ thresholds are shown by bars and dashed lines, respectively, for the *N* (blue), *E* (orange), and *Z* (yellow) components.

The mechanisms that generated the observed anomalies need to be clarified to completely understand the phenomenon of pre-earthquake electromagnetics (also known as seismo-electromagnetics). The change of conductivity in the underground is a possible mechanism since past studies have reported such change prior to earthquakes (Manga et al., 2003). Dehydrated crustal rocks have a weak electrical conductivity under the normal condition because the conductivity largely depends on the dynamics of underground fluid and how it is distributed. As microcracks are being formed in the rocks during the earthquake preparation phase, underground fluid could migrate to different locations. The process could alter distribution of the fluid as well as modify the underground conductivity which subsequently generate anomalies in the geomagnetic field (Hayakawa, 2015). Additionally, it is estimated that M6.0+ earthquakes would be able to generate magnetic signals via the induction of electromagnetic field that are detectable from more than 100 km away, and via electrokinetic effects that can be detected from more than 200 km away (Hayakawa, 2015). Hence, it was assumed based on these estimations that the anomalies observed in this study were due to the superposition of both generation mechanisms.

Previous studies that employed the DVRR method mainly detected anomalies in the Z (e.g., Han et al., 2015; Han et al., 2016; Liu et al., 2006; Xu et al., 2013) that could be attributed to the highly responsive characteristic of the component toward signals propagating from nearby crusts since the signals carry substantial power perpendicular to the Earth's surface (Hattori et al., 2013). Thus, the mechanisms previously elaborated are adequate to clarify the majority of the results reported by previous studies as well as the observation regarding the Z component in the current study. In contrast, a different phenomenon was considered to explain the observations in the N and E components. Albeit much rarer, a phenomenon called ULF depression was discovered prior to earthquakes, reportedly affected only the horizontal component ($H^2 = N^2 + E^2$) (Potirakis et al., 2019a; Schekotov et al., 2006; Schekotov et al., 2020). The phenomenon is an effect of the decreased spectral power in the horizontal components due to the heightened Alfvén waves absorption propagating downward that is induced by radon gas emanated from the

earthquake epicenter (Hayakawa, 2015; Pulinets et al., 2018). Since the depression was manifested as the lack of waveform fluctuations in filtered signals (i.e., ULF with oscillation periods, $T \leq 100$ s) (Schekotov et al., 2006), it is theoretically possible that the total variation range could be significantly diminished if the depression happened during the period of maximum or/and minimum intensities of the typical diurnal variation.

The ULF depression phenomenon is 'highly sensitive' where it was claimed to be detectable at stations located as far as 400 km away from the epicenter due to its dependence on the ionosphere (Schekotov et al., 2020), which could spread out its perturbing effects over a greater coverage (Potirakis et al., 2019b). Hence, if anomalies in all geomagnetic components were generated through various channels several months before the earthquake, anomalies through a wide-reaching channel like the seismo-ionospheric effect were more likely to arrive at any observatory stations earlier. This assumption was based on how anomalies are generated underground where the process could start up to two months before earthquakes (Akinaga et al., 2001; Han et al., 2015; Han et al., 2016; Xu et al., 2013) and the generation occurs continuously instead of short-lived (Hayakawa, 2015). In addition, the direct lithospheric effect that potentially generated the *Z* component anomalies are said to be locally confined and has shorter detectable distances. Hence, the difference in terms of the mechanisms that generated *Z* and horizontal component anomalies is a possible explanation for the temporal lags of the anomaly appearances where the former appeared after the latter.

Conclusion

The study of statistical significance of diurnal variation anomalies in the geomagnetic field appearing before earthquakes was carried out for the first time by utilizing long-term data. Through this study, the DVRR method was found to be successful in minimizing solar disturbances while preserving possible seismically induced anomalies. It was found that all three components exhibited significant increases in anomaly counts, contrary to findings by previous studies where only anomalies in the *Z* component were observed. Based on the results and proposed mechanisms, the anomalies were verified to be significant as well as might be associated with the earthquakes and therefore were possibly precursors to the subsequent earthquakes. It is recommended for future studies to incorporate observations based on satellite data to expand the coverage of geomagnetic field data.

Acknowledgement

This work was supported in part by the Ministry of Higher Education Malaysia through Universiti Kebangsaan Malaysia under Grant FRGS/1/2020/TK0/UKM/01/1.

The magnetometer data were contributed by the following organizations: INTERMAGNET, Alan Thomson; CARISMA, PI Ian Mann; CANMOS, Geomagnetism Unit of the Geological Survey of Canada; The S-RAMP Database, PI K. Yumoto and Dr. K. Shiokawa; The SPIDR database; AARI, PI Oleg Troshichev; The MACCS program, PI M. Engebretson; GIMA; MEASURE, UCLA IGPP and Florida Institute of Technology; SAMBA, PI Eftyhia Zesta; 210 Chain, PI K. Yumoto; SAMNET, PI Farideh Honary; IMAGE, PI Liisa Juusola; Finnish Meteorological Institute, PI

Liisa Juusola; Sodankylä Geophysical Observatory, PI Tero Raita; UiT the Arctic University of Norway, Tromsø Geophysical Observatory, PI Magnar G. Johnsen; GFZ German Research Centre For Geosciences, PI Jürgen Matzka; Institute of Geophysics, Polish Academy of Sciences, PI Anne Neska and Jan Reda; Polar Geophysical Institute, PI Alexander Yahnin and Yarolav Sakharov; Geological Survey of Sweden, PI Gerhard Schwarz; Swedish Institute of Space Physics, PI Masatoshi Yamauchi; AUTUMN, PI Martin Connors; DTU Space, Thom Edwards and PI Anna Willer; South Pole and McMurdo Magnetometer, PI's Louis J. Lanzarotti and Alan T. Weatherwax; ICESTAR; RAPIDMAG; British Artarctic Survey; McMac, PI Dr. Peter Chi; BGS, PI Dr. Susan Macmillan; Pushkov Institute of Terrestrial Magnetism, Ionosphere and Radio Wave Propagation (IZMIRAN); MFGI, PI B. Heilig; Institute of Geophysics, Polish Academy of Sciences, PI Anne Neska and Jan Reda; University of L'Aquila, PI M. Vellante; BCMT, V. Lesur and A. Chambodut; Data obtained in cooperation with Geoscience Australia, PI Andrew Lewis; AALPIP, co-PIs Bob Clauer and Michael Hartinger; SuperMAG, PI Jesper W. Gjerloev; Data obtained in cooperation with the Australian Bureau of Meteorology, PI Richard Marshall; MAGDAS/CPMN, PI Akimasa Yoshikawa; International Center for Space Weather Science and Education, Kyushu University.

References

Akinaga, Y., Hayakawa, M., Liu, J. Y., Yumoto, K., & Hattori, K. (2001). A precursory ULF signature for the Chi-Chi earthquake in Taiwan. *Natural Hazards and Earth System Science, 1*(1), 33–36. https://doi.org/10.5194/nhess-1-33-2001

Chi, P. J., Engebretson, M. J., Moldwin, M. B., Russell, C. T., Mann, I. R., Hairston, M. R., Reno, M., Goldstein, J., Winkler, L. I., Cruz-Abeyro, J. L., Lee, D.-H., Yumoto, K., Dalrymple, R., Chen, B., & Gibson, J. P. (2013). Sounding of the plasmasphere by Mid-continent MAgnetoseismic Chain (McMAC) magnetometers. *Journal of Geophysical Research: Space Physics, 118*(6), 3077–3086. https://doi.org/10.1002/jgra.50274

Clauer, C. R., Kim, H., Deshpande, K., Xu, Z., Weimer, D., Musko, S., Crowley, G., Fish, C., Nealy, R., Humphreys, T. E., Bhatti, J. A., & Ridley, A. J. (2014). An autonomous adaptive low-power instrument platform (AAL-PIP) for remote high-latitude geospace data collection. *Geoscientific Instrumentation, Methods and Data Systems, 3*(2), 211–227. https://doi.org/10.5194/gi-3-211-2014

Engebretson, M. J., Hughes, W. J., Alford, J. L., Zesta, E., Cahill, L. J., Arnoldy, R. L., & Reeves, G. D. (1995). Magnetometer array for cusp and cleft studies observations of the spatial extent of broadband ULF magnetic pulsations at cusp/cleft latitudes. *Journal of Geophysical Research, 100*(A10), 371–386. https://doi.org/10.1029/95JA00768

Gjerloev, J. W. (2012). The SuperMAG data processing technique. *Journal of Geophysical Research: Space Physics, 117*(A9), 1-19. https://doi.org/10.1029/2012JA017683

Hamid, N. S. A., Rosli, N. I. M., Ismail, W. N. I., & Yoshikawa, A. (2021). Effects of solar activity on ionospheric current system in the Southeast Asia region. *Indian Journal of Physics, 95*(4), 543–550. https://doi.org/10.1007/s12648-020-01734-2

Han, P., Hattori, K., Hirokawa, M., Zhuang, J., Chen, C.-H., Febriani, F., Yamaguchi, H., Yoshino, C., Liu, J.-Y., & Yoshida, S. (2014). Statistical analysis of ULF seismomagnetic phenomena at

Kakioka, Japan, during 2001-2010. *Journal of Geophysical Research: Space Physics, 119*(6), 4998–5011. https://doi.org/10.1002/2014JA019789

Han, P., Hattori, K., Huang, Q., Hirooka, S., & Yoshino, C. (2016). Spatiotemporal characteristics of the geomagnetic diurnal variation anomalies prior to the 2011 Tohoku earthquake (Mw 9.0) and the possible coupling of multiple pre-earthquake phenomena. *Journal of Asian Earth Sciences, 129*(1), 13–21. https://doi.org/10.1016/j.jseaes.2016.07.011

Han, P., Hattori, K., Xu, G., Ashida, R., Chen, C.-H., Febriani, F., & Yamaguchi, H. (2015). Further investigations of geomagnetic diurnal variations associated with the 2011 off the Pacific coast of Tohoku earthquake (Mw 9.0). *Journal of Asian Earth Sciences, 114*, 321–326. https://doi.org/10.1016/j.jseaes.2015.02.022

Hattori, K., Han, P., Yoshino, C., Febriani, F., Yamaguchi, H., & Chen, C.-H. (2013). Investigation of ULF Seismo-Magnetic Phenomena in Kanto, Japan During 2000–2010: Case Studies and Statistical Studies. *Surveys in Geophysics, 34*(3), 293–316. https://doi.org/10.1007/s10712-012-9215-x

Hayakawa, M. (2015). *Earthquake Prediction with Radio Techniques.* Singapore: John Wiley & Sons Pte Ltd.

Hayakawa, M. (2018). Earthquake Precursor Studies in Japan. In D. Ouzounov, S. Pulinets, K. Hattori, & P. Taylor (Eds.), *Geophysical monograph: Vol. 234. Pre-Earthquake Processes. A Multidisciplinary Approach to Earthquake Predication Studies* (pp. 7–18). Hoboken: John Wiley & Sons, Inc.

Jordan, T. H., Chen, Y.-T., Gasparini, P., Madariaga, R., Main, I., Marzocchi, W., Papadopoulos, G., Sobolev, G., Yamaoka, K., & Zschau, J. (2011). Operational earthquake forecasting: State of knowledge and guidelines for utilization. *Annals of Geophysics, 54*(4), 316–391. https://doi.org/10.4401/ag-5350

Lichtenberger, J., Clilverd, M. A., Heilig, B., Vellante, M., Manninen, J., Rodger, C. J., Collier, A. B., Jørgensen, A. M., Reda, J., Holzworth, R. H., Friedel, R., & Simon-Wedlund, M. (2013). The plasmasphere during a space weather event: first results from the PLASMON project. *Journal of Space Weather and Space Climate, 3*, A23. https://doi.org/10.1051/swsc/2013045

Liu, J. Y., Chen, Y.-I., Chuo, Y. J., & Chen, C. S. (2006). A statistical investigation of pre-earthquake ionospheric anomaly. *Journal of Geophysical Research, 111*(A5), 1–5. https://doi.org/10.1029/2005JA011333

Love, J. J., & Chulliat, A. (2013). An International Network of Magnetic Observatories. *Eos, Transactions American Geophysical Union, 94*(42), 373–374. https://doi.org/10.1002/2013EO420001

Manga, M., Brodsky, E. E., & Boone, M. (2003). Response of streamflow to multiple earthquakes. *Geophysical Research Letters, 30*(5), 181-183. https://doi.org/10.1029/2002GL016618

Mann, I. R., Milling, D. K., Rae, I. J., Ozeke, L. G., Kale, A., Kale, Z. C., Murphy, K. R., Parent, A., Usanova, M., Pahud, D. M., Lee, E.-A., Amalraj, V., Wallis, D. D., Angelopoulos, V., Glassmeier, K.-H., Russell, C. T., Auster, H.-U., & Singer, H. J. (2008). The Upgraded CARISMA Magnetometer Array in the THEMIS Era. *Space Science Reviews, 141*(1-4), 413–451. https://doi.org/10.1007/s11214-008-9457-6

Masci, F., & Thomas, J. N. (2015). Are there new findings in the search for ULF magnetic precursors to earthquakes? *Journal of Geophysical Research: Space Physics, 120*(12), 10289–10304. https://doi.org/10.1002/2015JA021336

Potirakis, S. M., Contoyiannis, Y., Koulouras, G. E., Melis, N. S., Eftaxias, K., & Nomicos, C. (2019a). *Pre-earthquake electromagnetic emissions with critical and tricritical behavior before the recent Durrës (Albania) (Mw=6.4, 26-11-2019) and Chania (Greece) (Mw=6.1, 27-11-2019) earthquakes.* https://arxiv.org/pdf/1912.05955

Potirakis, S. M., Hayakawa, M., & Schekotov, A. (2017). Fractal analysis of the ground-recorded ULF magnetic fields prior to the 11 March 2011 Tohoku earthquake (Mw=9): discriminating possible earthquake precursors from space-sourced disturbances. *Natural Hazards, 85*(1), 59–86. https://doi.org/10.1007/s11069-016-2558-8

Potirakis, S. M., Schekotov, A., Contoyiannis, Y., Balasis, G., Koulouras, G. E., Melis, N. S., Boutsi, A. Z., Hayakawa, M., Eftaxias, K., & Nomicos, C. (2019b). On Possible Electromagnetic Precursors to a Significant Earthquake (Mw = 6.3) Occurred in Lesvos (Greece) on 12 June 2017. *Entropy (Basel, Switzerland), 21*(3), 241. https://doi.org/10.3390/e21030241

Pulinets, S., Ouzounov, D., Karelin, A., & Davidenko, D. (2018). Lithosphere-Atmosphere-Ionosphere-Magnetosphere Coupling-A Concept for Pre-Earthquake Signals Generation. In D. Ouzounov, S. Pulinets, K. Hattori, & P. Taylor (Eds.), *Geophysical monograph: Vol. 234. Pre-Earthquake Processes. A Multidisciplinary Approach to Earthquake Predication Studies* (pp. 77–98). Hoboken: John Wiley & Sons, Inc.

Rostoker, G. (1972). Geomagnetic indices. *Reviews of Geophysics, 10*(4), 935–950. https://doi.org/10.1029/RG010i004p00935

Samson, J. C., & Yeung, K. L. (1986). Some generalizations on the method of superposed epoch analysis. *Planetary and Space Science, 34*(11), 1133–1142. https://doi.org/10.1016/0032-0633(86)90025-5

Schekotov, A., Chebrov, D., Hayakawa, M., Belyaev, G. G., & Berseneva, N. (2020). Short-term earthquake prediction in Kamchatka using low-frequency magnetic fields. *Natural Hazards, 100*(2), 735–755. https://doi.org/10.1007/s11069-019-03839-2

Schekotov, A., Molchanov, O. A., Hattori, K., Fedorov, E. N., Gladyshev, V. A., Belyaev, G. G., Chebrov, V. N., Sinitsin, V., Gordeev, E., & Hayakawa, M. (2006). Seismo-ionospheric depression of the ULF geomagnetic fluctuations at Kamchatka and Japan. *Physics and Chemistry of the Earth, Parts A/B/C, 31*(4-9), 313–318. https://doi.org/10.1016/j.pce.2006.02.043

Singh, Y. P., & Badruddin (2006). Statistical considerations in superposed epoch analysis and its applications in space research. *Journal of Atmospheric and Solar-Terrestrial Physics, 68*(7), 803–813. https://doi.org/10.1016/j.jastp.2006.01.007

Tanskanen, E. I. (2009). A comprehensive high-throughput analysis of substorms observed by IMAGE magnetometer network: Years 1993-2003 examined. *Journal of Geophysical Research, 114*(A5), 1-11. https://doi.org/10.1029/2008JA013682

Xu, G., Han, P., Huang, Q., Hattori, K., Febriani, F., & Yamaguchi, H. (2013). Anomalous behaviors of geomagnetic diurnal variations prior to the 2011 off the Pacific coast of Tohoku earthquake (Mw9.0). *Journal of Asian Earth Sciences, 77*(1), 59–65. https://doi.org/10.1016/j.jseaes.2013.08.011

Yumoto, K. (2001). Characteristics of Pi 2 magnetic pulsations observed at the CPMN stations: A review of the STEP results. *Earth, Planets and Space, 53*(10), 981–992. https://doi.org/10.1186/BF03351695

Yusof, K. A., Abdullah, M., Hamid, N. S. A., Ahadi, S., & Yoshikawa, A. (2020). Normalized polarization ratio analysis for ULF precursor detection of the 2009 M7.6 Sumatra and 2015 M6.8 Honshu Earthquakes. *Jurnal Kejuruteraan, 3*(1), 35–41. https://doi.org/10.17576/jkukm-2020-si3(1)-06

Yusof, K. A., Abdullah, M., Hamid, N. S. A., Ahadi, S., & Yoshikawa, A. (2021). Correlations between Earthquake Properties and Characteristics of Possible ULF Geomagnetic Precursor over Multiple Earthquakes. *Universe, 7*(1), 20. https://doi.org/10.3390/universe7010020

Yusof, K. A., Hamid, N. S. A., Abdullah, M., Ahadi, S., & Yoshikawa, A. (2019). Assessment of signal processing methods for geomagnetic precursor of the 2012 M6.9 Visayas, Philippines earthquake. *Acta Geophysica, 142*(67), 1297–1306. https://doi.org/10.1007/s11600-019-00319-w

Zhu, K., Li, K., Fan, M., Chi, C., & Yu, Z. (2019). Precursor Analysis Associated With the Ecuador Earthquake Using Swarm A and C Satellite Magnetic Data Based on PCA. *IEEE Access, 7*, 93927–93936. https://doi.org/10.1109/ACCESS.2019.2928015